Property modelling

Fast and reliable meta-data model for the mechanistic analysis of NR vulcanized with sulphur

G. Milani [a,*], F. Milani [b]

[a] Politecnico di Milano, Piazza Leonardo da Vinci 32, 20133 Milano, Italy
[b] CHEM. CO Consultant, Via J.F. Kennedy 2, 45030 Occhiobello, Rovigo, Italy

Article history:
Received 21 October 2013
Accepted 8 November 2013

1. Introduction

Sulphur vulcanization is the most practical and popular method utilized in the rubber industry to cure items. To improve efficiency, sulphur is used in combination with one or more accelerators, as well as many activator systems such as, for instance, soluble zinc salts, fatty acids and other components, in addition to many fillers [1–7].

The quality of a cured item depends on several concurrent factors, as for instance the elastomer type, the concentration of active double bonds, the quality of all the components (including filler) and their concentrations. When dealing with natural rubber (NR), a decrease in the vulcanizate properties – commonly known as reversion, Fig. 1, is experienced at long curing times, especially at high temperatures. Chen and co-workers [8] have shown that

* Corresponding author. Tel.: +39 3495516064.
E-mail addresses: gabriele.milani77@gmail.com, gabriele.milani@polimi.it (G. Milani), federico-milani@libero.it (F. Milani).

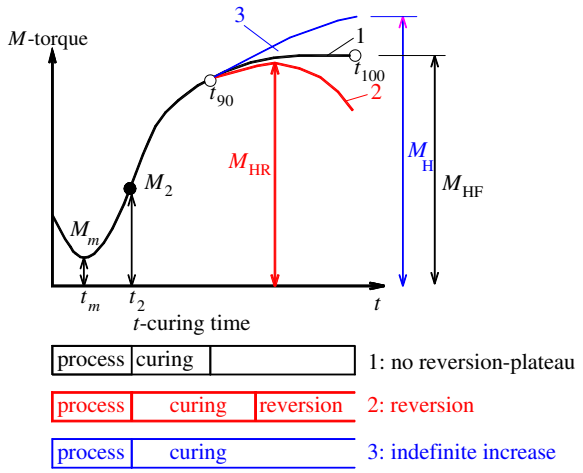

Fig. 1. Typical experimental behaviour of a rubber compound during a rheometer test.

this phenomenon seems to appear when two reactions are competing during vulcanization. Loo [9] demonstrated that, as the cure temperature rises, the crosslink density drops, thus increasing the degree of reversion. Morrison and Porter [10] confirmed that the observed reduction in vulcanizate properties is caused by two reactions proceeding in parallel, i.e. de-sulphuration and decomposition (see Fig. 2).

Recently, some valuable advances in the construction of simplified but effective mathematical models have been achieved by different authors, including Ding and Leonov [11], Ding et al. [12], Milani et al. [13–17] and Leroy et al. [18].

In this framework, relatively simple kinetic models to interpret rubber vulcanized with sulphur through rheometer curves have been proposed very recently, e.g. [16–18]. All the models are based on rheometer curves data fitting and require having a huge number of data points at the experimenter's disposal, possibly at different temperatures, in order to obtain model parameters, usually thorough standard least squares routines.

A kinetic approach [16–18] has the advantage of allowing an estimation of partial reaction kinetic constants, eventually at increasing temperatures, providing interesting information on the behaviour of a blend in the presence of different co-agents and curing conditions. Its main limitation is the complexity of the model itself, which requires the determination of several unknown variables through non-linear least squares fitting, and the subsequent need to have several data points in hand in order to obtain reliable estimates of the unknowns.

The aim of the present paper is, therefore, to kinetically characterize NR blends while having only limited information available on the behaviour of the materials under standard rheometer tests, by means of a simplified but still effective mechanistic model. Such a situation is typical for many practitioners faced with the problem of optimizing a vulcanization process with only minimal information provided by the blend sellers.

The approach proposed consists of two steps, the first characterized by constructing experimental meta-data from limited rheometer information, and the second by determining the partial reaction kinetics at the base of the vulcanization process, assuming the experimental data fits with that obtained in the previous phase using the meta-model.

To assess the results obtained with the proposed model, a number of cases were analysed using the same NR blend in the presence of different accelerators at variable concentrations, with only a few specifics available from the literature; the same modelling was also run in the presence of moderate and strong reversion.

The procedure proved to be very fast and reliable and had the advantage of providing, for the single cases analysed, partial reaction kinetic constants. This knowledge allows, at least in principle, the behaviour of a blend to be predicted under different thermal conditions, without the need to perform a costly series of experiments.

The approach is generalizable and can be used in the presence of any rubber compound, provided that suitable but limited experimental data are available to characterize curing at different temperatures.

2. Essential data to build meta-data from rheometer curves

The standard experimental test to evaluate macroscopically the vulcanization characteristics of vulcanizable rubber is the rheometer test [19], where the elastic torque response M is measured. During torque-time measures, as illustrated in Fig. 1, three different situations can occur: (a) the curve reaches a maximum asymptotically, (b) the curve reaches a maximum and then decreases (reversion) and (c) the curve increases monotonically after the scorch time t_2. Case (c) is rarely encountered in practice, especially for NR.

In Fig. 1, we define the following characteristic times: t_m (minimum torque point), t_2 (scorch or time to incipient cure), t_{90} (time at a degree of vulcanization equal to 90%) and t_{100} (end of experimentation, torque equal to M_{HF}).

Rubber producers usually furnish only values for t_m (not strictly necessary to kinetically identify the blend), t_2, t_{90} and t_{100} or, more frequently, the reversion percentage instead of t_{100}. It will be shown in the following Sections that the application of a combined procedure whereby a three-function spline and the subsequent application of a mechanistic model based on meta-data obtained in the previous step allows fast and reliable estimation of kinetic constants, where minimal data are available from a quick characterization of the blend from a thermal standpoint, usually the only data available industrially.

3. Meta-data generation: natural cubic splines vs. three-function experimental data interpolation

A new approach to a fast meta-data approximation starting from knowledge of a few "characteristic" experimental points on the rheometer curve (when the entire cure curve is not available) is presented here. The procedure is based on a natural cubic spline interpolation of the experimental data at hand, which typically include t_m, t_2, t_{90}, t_{100}, M_m, M_2, M_{90} and M_{HF} (see Fig. 1). Instead of M_{HF} the reversion percentage, i.e. the decrease in the peak torque at the end of the rheometer test, may be provided.

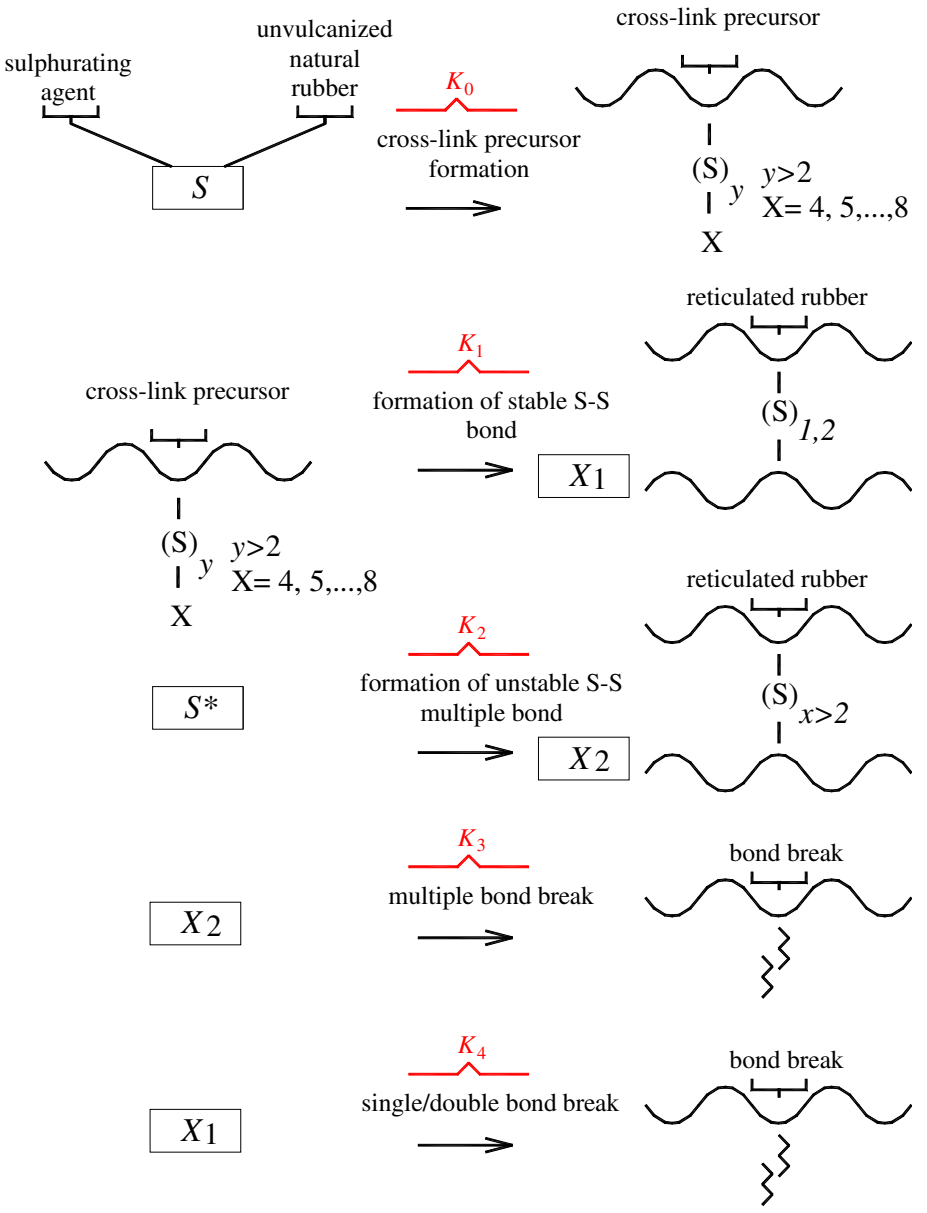

Fig. 2. Products and schematic reaction mechanisms of NR accelerated sulphur vulcanization.

3.1. Composite three-function C_1 interpolation

In [14,15], a fast heuristic model to obtain meta-data in the absence of a full rheometer curve has been proposed. The mathematical approximation used in [14,15] relies upon approximating experimental data with a three-function composite first derivative continuous (C_1) curve represented by two parabolas and a rectangular hyperbola, with asymptotes either unrotated [14] or rotated [15] through a pre-determined ϑ angle with respect to the horizontal axis to represent reversion.

Only four points on the experimental cure curve are needed, namely t_m, t_2, t_{90} and the angle of reversion. The first parabola holds in the time range between zero and t_2, the second parabola between t_2 and t_{90} and the hyperbola after t_{90}.

General equations used to characterize the three-function curve are:

$$\begin{aligned} M(t) &= a_1 t^2 + b_1 t + c_1 \\ t(M) &= a_2 M^2 + b_2 M + c_2 \\ M^2 + M\left(\tfrac{t}{\tan\vartheta} - t\tan\vartheta + a_3 + b_3\right) + \left(-t^2 - a_3 t\tan\vartheta + \tfrac{b_3 t}{\tan\vartheta} + a_3 b_3 - c_3\right) &= 0 \end{aligned} \tag{1}$$

Constants a_1, b_1 and c_1 of the first parabola (with vertical axis) are determined by imposing passage of the curve through the scorch point and assuming the vertex in t_m (three algebraic conditions).

The second parabola (with horizontal axis) is determined by imposing passage through t_2 and t_{90} and assuming that the first and second parabolas have the same first derivative in t_2, i.e. $(2a_1t_2 + b_1) = (2a_2M_2 + b_2)^{-1}$.

Finally, the hyperbola is analytically determined by imposing (i) passage through t_{90}, (ii) a common tangent in t_{90} with the second parabola and (iii) a passage condition through a further point, for instance $(t_{100}; M_{HF})$. It is worth underlining that the asymptotic rotation angle ϑ has to be chosen a-priori via a-posteriori evaluation of the fitting performance of reversion. Finally, it is worth noting that the model is sufficiently general to also reproduce horizontal plateaus (ideal behaviour without reversion) and indefinitely increasing cure curves.

3.2. Natural cubic spline C_2 interpolation

The natural cubic spline procedure adopted here provides results in better agreement with the real behaviour of NR under curing when compared to [14,15] because it is a second derivative continuous (C_2) approach.

The fundamental idea behind cubic spline interpolation is based on the engineer's tool used to draw smooth curves through a number of points of the actual rheometer curve $M(t)$.

Spline interpolation is based on the following hypotheses:

1. The piecewise function $M(t)$ interpolates all data points.
2. $M(t)$ together with its first and second derivatives ($M'(t)$ and $M''(t)$ respectively) are continuous on the interval $[0 \quad t_{max}]$.

The kernel relies on the fitting of known experimental points at times t_1, t_2,…,t_n by means of a piecewise function of the form:

$$M(t) = \begin{cases} M_1(t) & \text{if} \quad t_1 \le t \le t_2 \\ M_2(t) & \text{if} \quad t_2 \le t \le t_3 \\ \dots & \\ M_{n-1}(t) & \text{if} \quad t_{n-1} \le t \le t_n \end{cases} \tag{2}$$

where M_i are third degree polynomial functions defined as:

$$M_i(t) = a_i(t - t_i)^3 + b_i(t - t_i)^2 + c_i(t - t_i) + d_i \quad i = 1, 2, \dots, n-1 \tag{3}$$

First and second derivatives of Eq. (3) are:

$$dM_i(t)/dt = 3a_i(t - t_i)^2 + 2b_i(t - t_i) + c_i \quad d^2M_i(t)/dt^2 = 6a_i(t - t_i) + 2b_i \tag{4}$$

Assuming that the composite function passes through experimental points (say that, at t_i, the rheometer curve has a torque equal to $\overline{M}_i$), and it is continuous with its first and second derivatives (equal to $\overline{M}_i'$ and $\overline{M}_i''$ in t_i, respectively), we obtain $2n-2$ mathematical conditions for the passage through experimental points and $2(n-2)$ conditions for the first and second derivative continuity, respectively.

The total coefficients to be set are $4(n-1)$, so that the number of coefficients exceeds the equality conditions by 2 equations.

We assume, for the sake of simplicity and also in agreement with the actual behaviour of rubber as experienced in the rheometer, a so-called "natural" spline

Table 1
Composition of the model rubber compound used to validate the first-step, i.e. meta-experimental data generation, from [17].

Component	phr
Rubber gum	100
Carbon black	25
Oil	5
(ZnO/Stearic acid) activator	6
Sulphur	3
Amine antioxidant	2

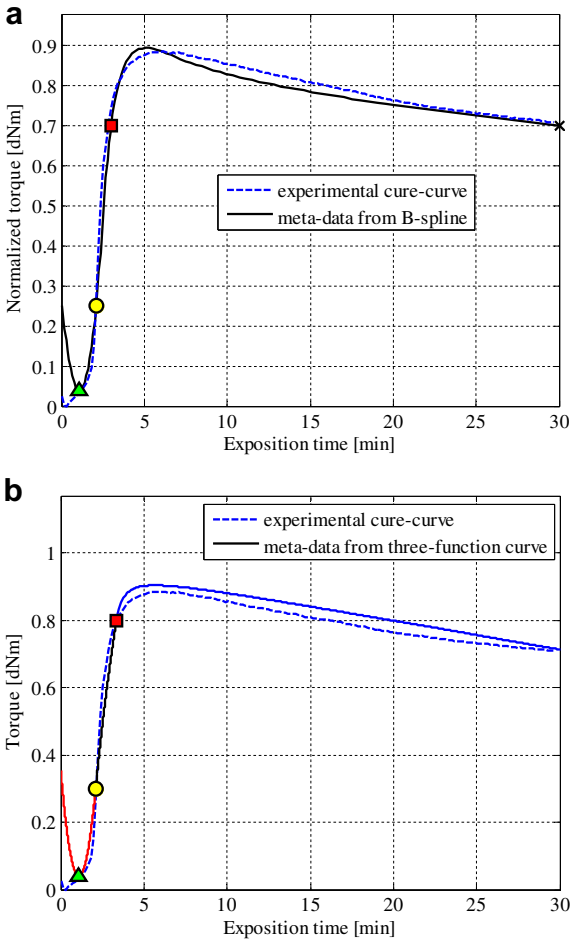

Fig. 3. NR at 170 °C. Comparison between experimental normalized cure curve and numerically generated meta data using points indicated in the figure with squares, triangles, circles and crosses. a: B-spline meta data; b: three-function composite curve.

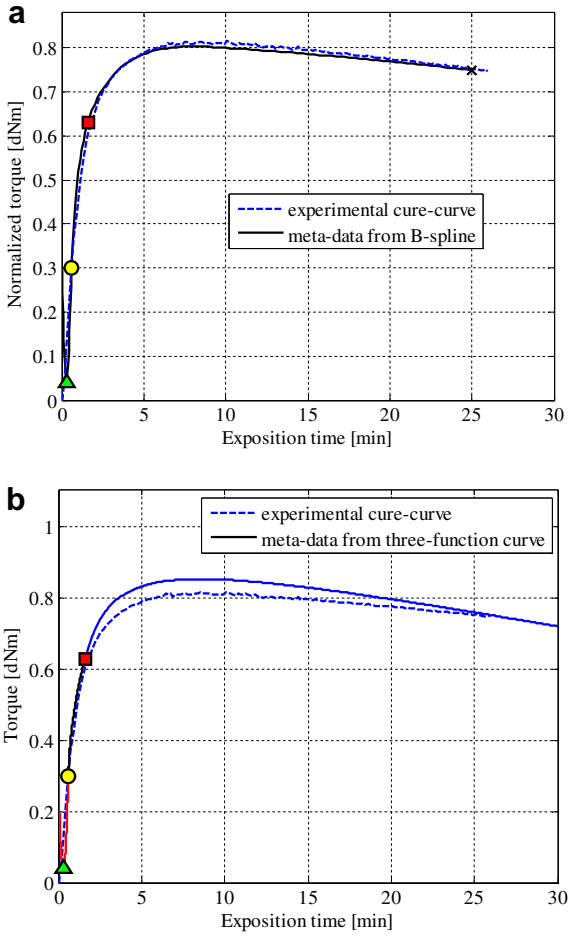

Fig. 4. NR at 160 °C. Comparison between experimental normalized cure curve and numerically generated meta data using points indicated in the figure with squares, triangles, circles and crosses. a: B-spline meta data; b: three-function composite curve.

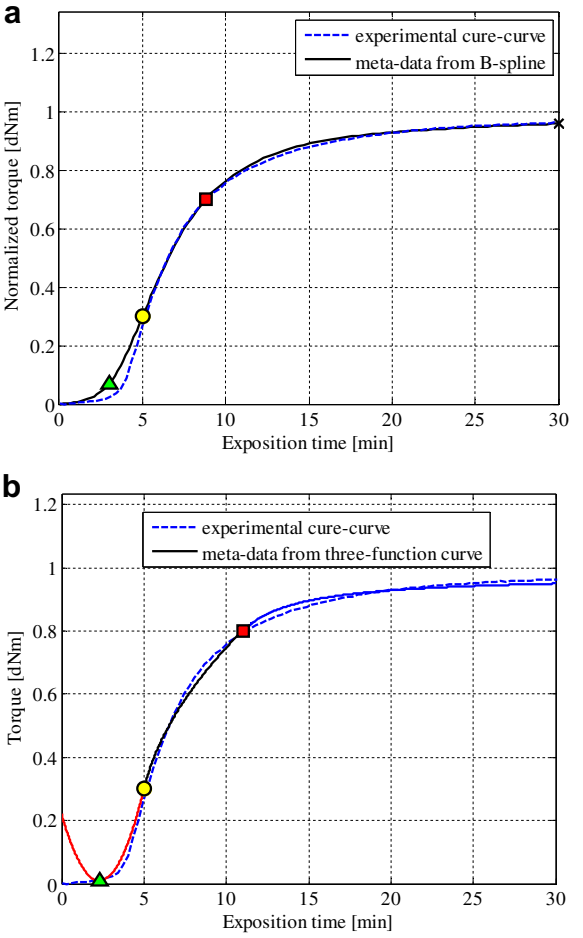

Fig. 5. NR at 140 °C. Comparison between experimental normalized cure curve and numerically generated meta data using points indicated in the figure with squares, triangles, circles and crosses. a: B-spline meta data; b: three-function composite curve.

formulation, which assumes that the second derivatives at the end points are equal to zero, namely $\overline{M}_1'' = \overline{M}_n'' = 0$.

In this latter case, the following system of equations is required to find a_i, b_i, c_i and d_i:

$$2b_i - 6a_{i-1}h_i = 0 \tag{5a}$$

$$-\left(3a_{i-1}h_i^2 + 2b_{i-1}h_i\right) + c_i = 0 \tag{5b}$$

$$-\left(a_{i-1}h_i^3 + b_{i-1}h_i^2 + c_{i-1}h_i + d_{i-1}\right) + d_i = 0 \tag{5c}$$

$$d_i = \overline{M}_i \tag{5d}$$

Having defined with h_i the quantity $h_i = t_i - t_{i-1}$.

Equation (5)-a is the second derivative continuity, equation (5)-b the first derivative continuity, equation (5)-c the function continuity and (5)-d the passage through experimental points $\overline{M}_i$.

To test the performance of the model, the NR blend tested in [17,18], for which full cure-curves are in hand, is hereafter re-considered.

In [17,18], the isothermal cure of a natural rubber compound (Table 1) was studied at five different temperatures (130, 140, 150, 160 and 170 °C). The average M(t) curves obtained were used to calculate the evolution of the degree of vulcanisation $\alpha_{exp}(t)$ [20] using the relation:

Table 2
Composition of the NR compound to validate the two-step approach proposed, from [24].

Component	phr
Natural Rubber (SMR 5CV)	100
N330 Carbon black	50
Naphthenic oil	5
Stearic acid	6
Sulphur	2
ZnO	5

Table 3
Typology of accelerators used in [24] to test the activities of different accelerators in NR vulcanization.

MBTS	Benzothiazyl disulfide
MBS	N-oxydiethhylen-2-benzothiazyl-sulfenamide
TBBS	N-t-butyl-2-benzothiazyl-sulfenamide
TSSR	2-ethylamino-4-diethylamino-6-heptyldithio-sym-triazine
PYSSPY	2,2′-dithiobispyridine-N-oxide
TSST	Bis-(2-ethylamino-4-diethylamino-6-sym-triazinyl)disulfide
PSSR	Beta-(di-n-butylphosphorodithioylthio)-propionic acid, methyl ester
TBBS	N-t-butyl-2-benzothiazyl-sulfenamide
ZDBDP	Zinc O,O-di-n-butylphosphorodithioate
CTP	N-(cyclohexylthio)phthalimide

$$\alpha_{\exp}(t) = \frac{M(t) - M_{\min T}}{M_{\max T_0} - M_{\min T_0}} \tag{6}$$

where:

- $M_{\min T}$ is the minimum value of torque $M(t)$ during a cure experiment at temperature T. Before reaching this minimum value, $\alpha_{\exp}$ is considered equal to zero.
- $M_{\min T0}$ and $M_{\max T0}$ are the minimum and maximum torque values obtained for a cure experiment at a temperature T_0 low enough to allow reversion to be neglected.

In this way, the rheometer curves to fit always range between 0 and 1, with a maximum torque sensibly less than 1 for high vulcanization temperatures.

In what follows, only three of the five cure temperatures are considered for the sake of brevity, namely 170 °C, 160 °C and 140 °C. At 170 °C, reversion is considerable while at 160 °C there is a moderate drop in the degree of vulcanization; at 140 °C, negligible reversion is experienced.

The aim of the present comparison is to select only a few points on the experimental rheometer curves (indicated with different symbols in the relevant figures) to generate meta-data, either with a natural cubic splines approach or a composite three-function procedure [14,15], and finally to compare the meta-data thus generated with the whole experimental rheometer chart for a-posteriori assessment.

The meta-data curves are compared with the normalized experimental results in Figs. 3–5 at 170 °C, 160 °C and 140 °C, respectively.

As can be noted, both models fit the experimental evidence reasonably well, even with only a few fitting points. It is worth emphasizing that, in both models, it is not strictly necessary to utilize "characteristic points" on the rheometer chart, as for instance (t_{90}, M_{90}), but any data belonging to the experimental response may be used. The accuracy of the approximation depends, however, on the number and position of the points used, this being the crucial issue for a realistic representation of the vulcanization process.

Table 4
Literature data set 1, characteristic points on the rheometer curve and mechanical properties of the vulcanized items.

Label	1-1	1-2	1-3
S	2.5	2.5	2.5
Accelerator	TBBS 0.6	TBBS 0.2 ZDBDF 0.76	TBBS 0.2 ZDBDF 0.76 CTP 0.72
# Numerical simulation	1	2	3
t_2 scorch time [min] 144 °C	8.7	5.7	14.7
$t_{90}-t_2$ [min] 144 °C	10.8	6.3	7.3
Reversion % 160 °C	19.5	5.6	6.5
Cure time [min]	23.0	13.0	24.0
Mechanical properties, cure 144 °C			
M_{300} [MPa]	15.6	13.0	13.2
UTS [MPa]	29.5	28.0	28.0
UE [%]	542	555	550

Note.
M_{300}: elastic modulus at elongation equal to 300%.
UTS: ultimate tensile strength.
UE: elongation at break.

Table 5
Literature data set 2, characteristic points on the rheometer curve and mechanical properties of the vulcanized items.

Label	2-1	2-3	2-4
Accelerator	TBBS 0.6	TSST 0.7	TSSR 0.7
# Numerical simulation	1	4	5
t_2 scorch time [min] 144 °C	9.8	7.8	10.5
$t_{90}-t_2$ [min] 144 °C	12.8	17.2	21.2
Reversion % 160 °C	21.0	6.1	12.1
Cure time [min]	26.0	29.0	36.5
Mechanical properties, cure 144 °C			
M_{300} [MPa]	14.0	15.5	14.5
UTS [MPa]	27.5	28.0	28.0
UE [%]	517	503	499

Note.
M_{300}: elastic modulus at elongation equal to 300%.
UTS: ultimate tensile strength.
UE: elongation at break.

4. Second step: mechanistic model fitting meta-data

In the second step, a mechanistic model fitting the meta-data obtained in the previous step is utilized to deduce kinetic constants underlying the partial reactions characterizing the degree of vulcanization. This knowledge of partial reaction kinetic constants is crucial when

Table 6
Literature data set 3, characteristic points on the rheometer curve and mechanical properties of the vulcanized items.

Label	3-1	3-2	3-4	3-6
Accelerator	TBBS 0.6	TSSR 1.0	TSSR 0.5 PSSR 0.5	PSSR 1.0
# Numerical simulation	1	6	7	8
t_2 scorch time [min] 144 °C	9.3	9.5	9.5	15.3
$t_{90}-t_2$ [min] 144 °C	12.8	16.0	13.0	22.3
Reversion % 160 °C	18.6	9.5	5.7	9.0
Cure time [min]	25.0	30.0	26.0	43.0
Mechanical properties, cure 144 °C				
M_{300} [MPa]	14.7	14.3	16.8	11.6
UTS [MPa]	28.4	27.1	27.1	25.0
UE [%]	508	510	464	544

Note.
M_{300}: elastic modulus at elongation equal to 300%.
UTS: ultimate tensile strength.
UE: elongation at break.

Table 7
Literature data set 4, characteristic points on the rheometer curve and mechanical properties of the vulcanized items.

Label	4-1	4-4	4-5	4-7
S	2.5	2.5	2.5	2.5
Accelerator	TBBS 0.6	MBS 0.25 PYSSPY 1	MBTS 1.0	PYSSPY 1.0
# Numerical simulation	1	9	10	11
t_2 scorch time [min] 144 °C	9.0	10.5	4.5	10.5
$t_{90}-t_2$ [min] 144 °C	13.2	14.7	13.2	31.8
Reversion % 160 °C	17.2	3.9	13.5	6.1
Cure time [min]	26.0	29.0	22.0	47.0
Mechanical properties, cure 144 °C				
M_{300} [MPa]	16.5	18.5	13.5	17.5
UTS [Mpa]	30.0	29.0	29.0	28.0
UE [%]	503	459	568	456

Note.
M_{300}: elastic modulus at elongation equal to 300%.
UTS: ultimate tensile strength.
UE: elongation at break.

Table 8
Literature data set 5, characteristic points on the rheometer curve and mechanical properties of the vulcanized items.

Label	5-2	5-3
S	2.5	2.5
Accelerator	MBTS 1.0	PYSSPY 1.0
# Numerical simulation	10	11
t_2 scorch time [min] 144 °C	4.8	11.3
$t_{90}-t_2$ [min] 144 °C	12.3	38.0
Reversion % 160 °C	20.8	6.9
Cure time [min]	20.5	54.5
Mechanical properties, cure 144 °C		
M_{300} [MPa]	10.2	12.6
UTS [MPa]	26.0	24.0
UE [%]	581	499

Note.
M_{300}: elastic modulus at elongation equal to 300%.
UTS: ultimate tensile strength.
UE: elongation at break.

Table 9
Overview of the experimental data utilized to validate the two-step numerical model (1/2).

Numerical test #	1	10	5	6	11	9
Label	Average 1-1 2-1 3-1 4-1	Average 4-5 5-2	2-4	3-2	Average 4-7 5-3	4-4
Reversion %	19.1	17.1	12.1	9.5	6.5	3.9
M_{300} [MPa]	15.2	11.8	14.5	14.3	15.0	18.5
UST [MPa]	28.8	27.5	28	27.1	26.0	29.0
UE [%]	517	574	499	510	477	459
Cure time [min] ODR 144 °C	25	21.2	36.5	30.0	50.7	29
t_2 [min]	9.2	4.65	10.5	9.5	10.9	10.5
t_{90} [min]	21.6	17.4	31.7	25.5	45.8	25.2
Product concentration in phr						
PYSSPY					1.0	1.0
MBS						0.25
TBBS	0.6					
TSSR			0.7	1.0		
MBTS		1.0				

Table 10
Overview of the experimental data utilized to validate the two-step numerical model (2/2).

Numerical test #	4	8	7	2	3
Label	2-3	3-6	3-4	1-2	1-3
Reversion %	6.1	9.0	5.7	5.6	6.5
M_{300} [MPa]	15.5	11.6	16.8	13.0	13.2
UST [MPa]	28.0	25.0	27.1	28.0	28.0
UE [%]	503	544	464	555	550
Cure time [min] ODR 144 °C	29	43	26	13	24
t_2 [min]	7.8	15.3	9.5	5.7	14.7
t_{90} [min]	25	37.6	22.5	12.0	22.0
Product concentration in phr					
TSST	0.7				
PSSR		1.0	0.5		
TSSR			0.5		
TBBS				0.2	0.2
ZDBDP				0.76	0.76
CTP					0.72

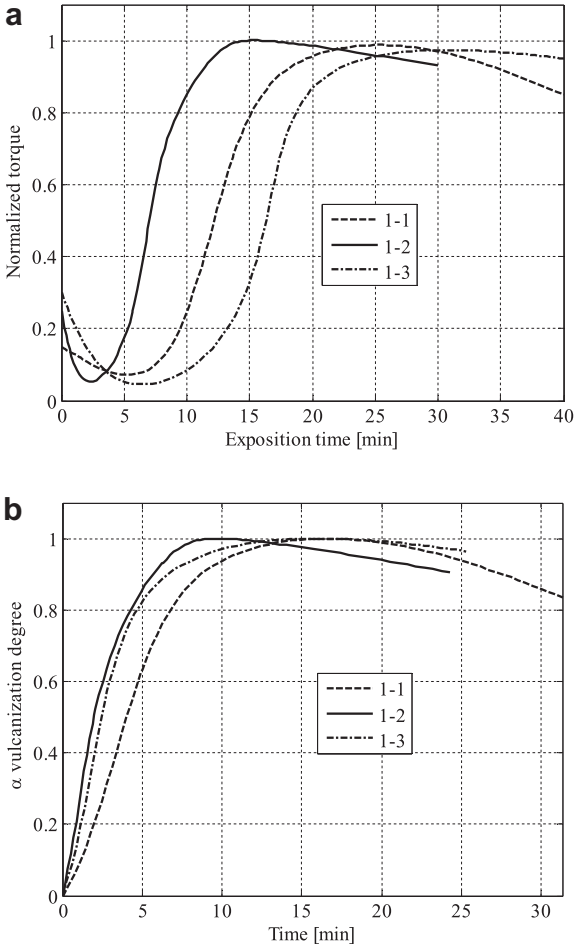

Fig. 6. Literature data set 1. a: spline meta-data; b: spline meta-data with exclusion of initial time interval before scorch.

numerical analysis of the curing behaviour of the blend under different thermal conditions is required.

A quite complex model for NR vulcanization requiring the iterated solution of an Ordinary Differential Equations System (ODES) has recently been proposed by the authors in [17]. In the present paper, a new approach is used, which simplifies the mathematical formulation [17] but allows deducing a closed form equation for the degree of vulcanization as a function of time, with the possibility of suitably representing reversion when appropriate.

The basic reaction schemes assumed in the present paper are shown in Fig. 2 and may be regarded at the same time as a simplification of the procedure proposed in [17] and a modification of classic models, with an increase in their complexity and accuracy level [21,22].

When compared with [17], the simplifications introduced rely upon a simpler mechanistic interpretation of reversion, without direct evaluation of primary and secondary back-biting, and less detailed modelling of the initial curing phase (precursor formation). In addition, the role played by accelerators is taken into account only in step one, i.e. in the meta-data.

There are five main reactions considered relevant, occurring in series and in parallel. The chain reaction is initiated by the formation of macro-radicals or macro-ions representing the intermediate cross-link precursor. Such a reaction is associated with a rate represented by the kinetic constant K_0.

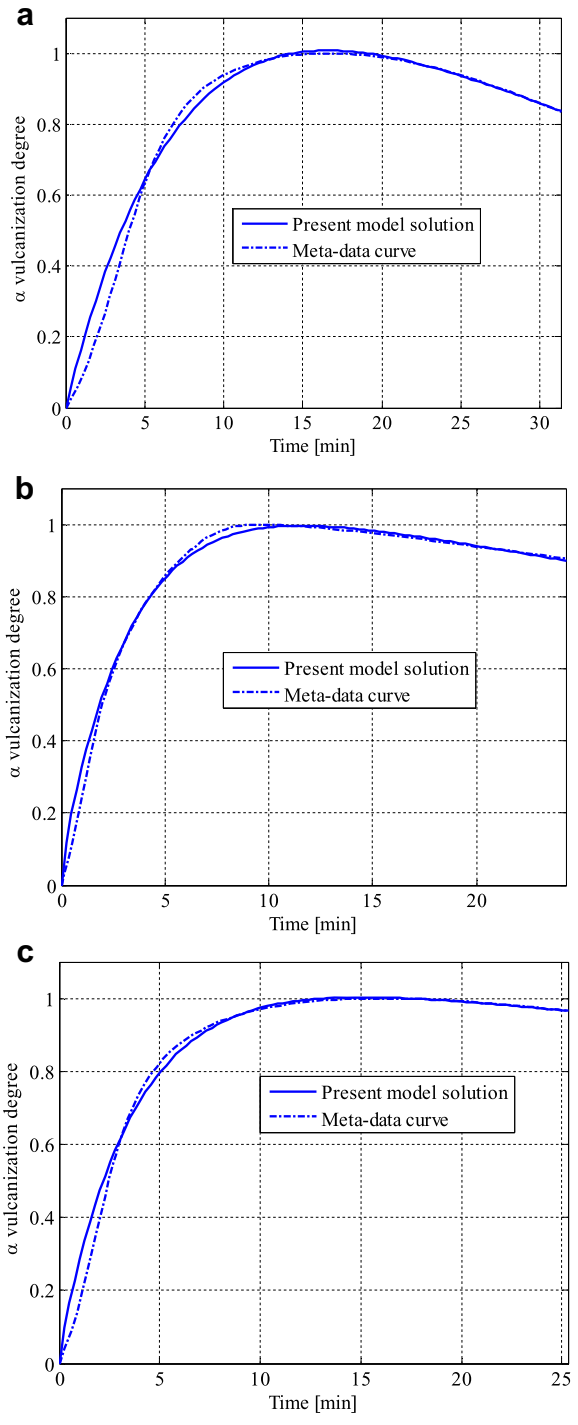

Fig. 7. Literature data set 1. a: 1-1 data set; b: 1-2 data set; c: 1-3 data set.

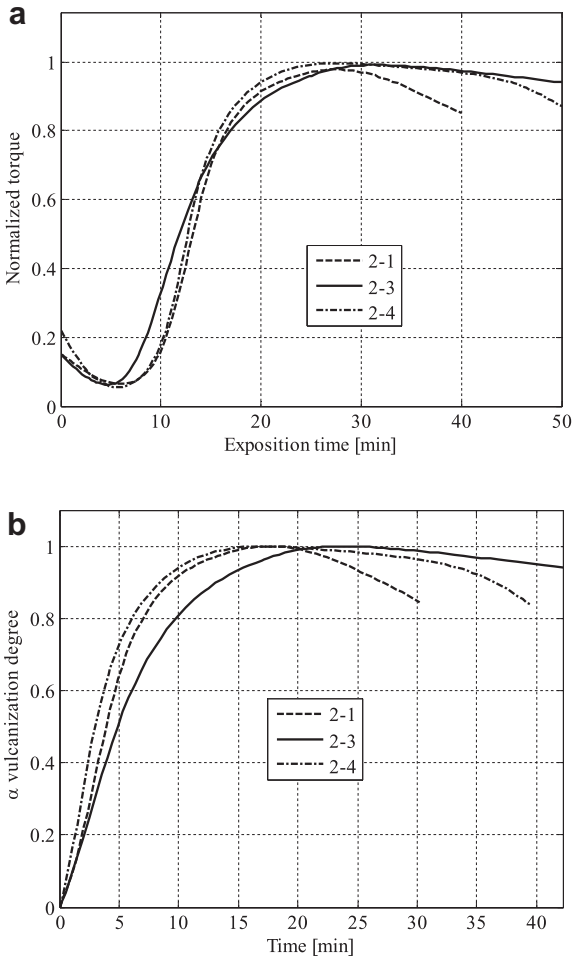

Fig. 8. Literature data set 2. a: spline meta-data; b: spline meta-data with exclusion of initial time interval before scorch.

The actual cross-linking proceeds through two pathways which have been shown to be additive, namely, the formation of more stable and unstable S-S bonds.

Since a multiple S-S bond is unstable, an immature crosslinked polymer evolves either to a mature crosslinked polymer exhibiting a single S or double bond between chains or to breakage of the bond, and hence devulcanization, which again occurs with backbiting of the bond in the same backbone chain. All these reactions occur with a kinetic rate dependent on the temperature reaction associated with three kinetic constants, K_1, K_2, and K_3.

Adopting the kinetic scheme constituted by the chemical reactions of Fig. 2, and already suggested by other authors for NR, see e.g. [21], the following schematization holds:

$$S \xrightarrow{k_0} S^* \qquad S^* \xrightarrow{k_1} X_1 \xrightarrow{k_4} D' \qquad S^* \xrightarrow{k_2} X_2 \xrightarrow{k_3} D \tag{7}$$

In Eq. (7), S is the uncured polymer, S^* the immature crosslinked polymer that evolves into the mature crosslinked polymer $X_1 + X_2$, with X_1 indicating the stable crosslinked portion and X_2 denoting the unstable part. Portions of both X_1 and X_2 may evolve into unvulcanized polymer, D and D', due to multiple S-S chain breaks and consequent backbiting. $K_{0,\ldots,4}$ are kinetic reaction constants.

The differential equations associated with the chemical reactions (7) are as follows:

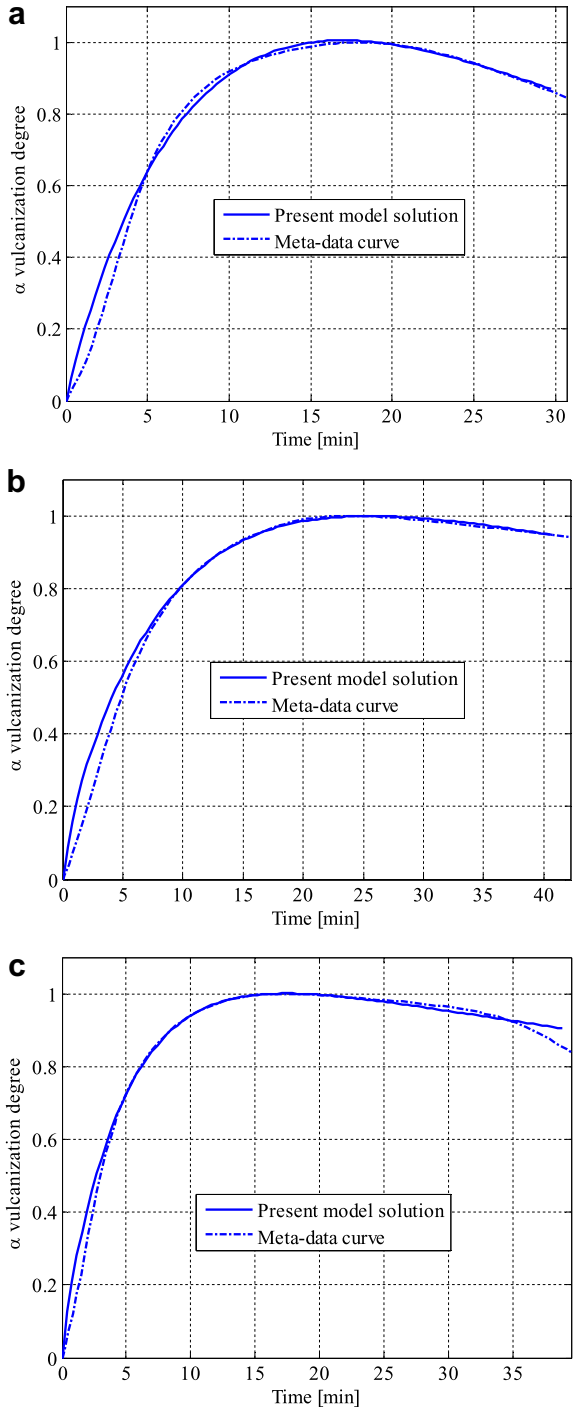

Fig. 9. Literature data set 2. a: 2-1 data set; b: 2-3 data set; c: 2-4 data set.

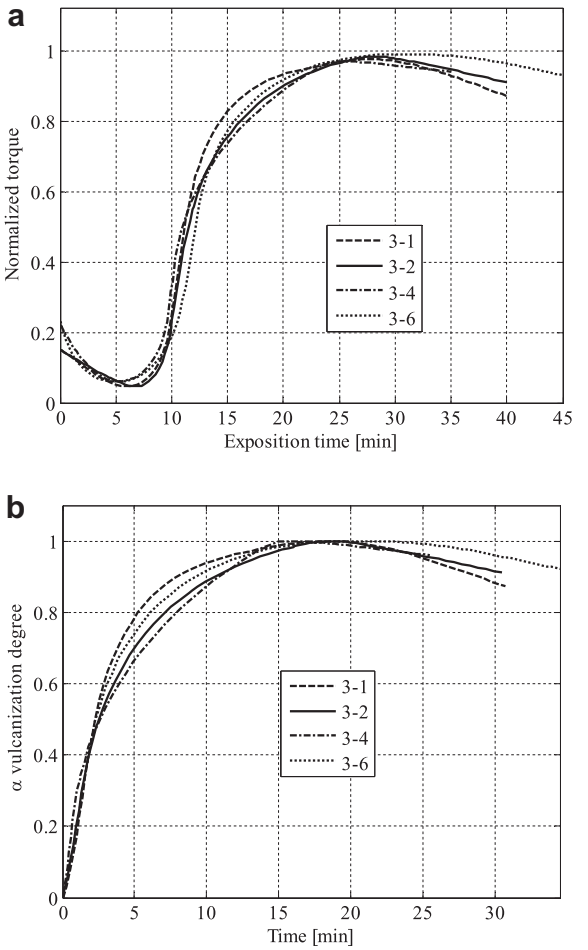

Fig. 10. Literature data set 3. a: spline meta-data; b: spline meta-data with exclusion of initial time interval before scorch.

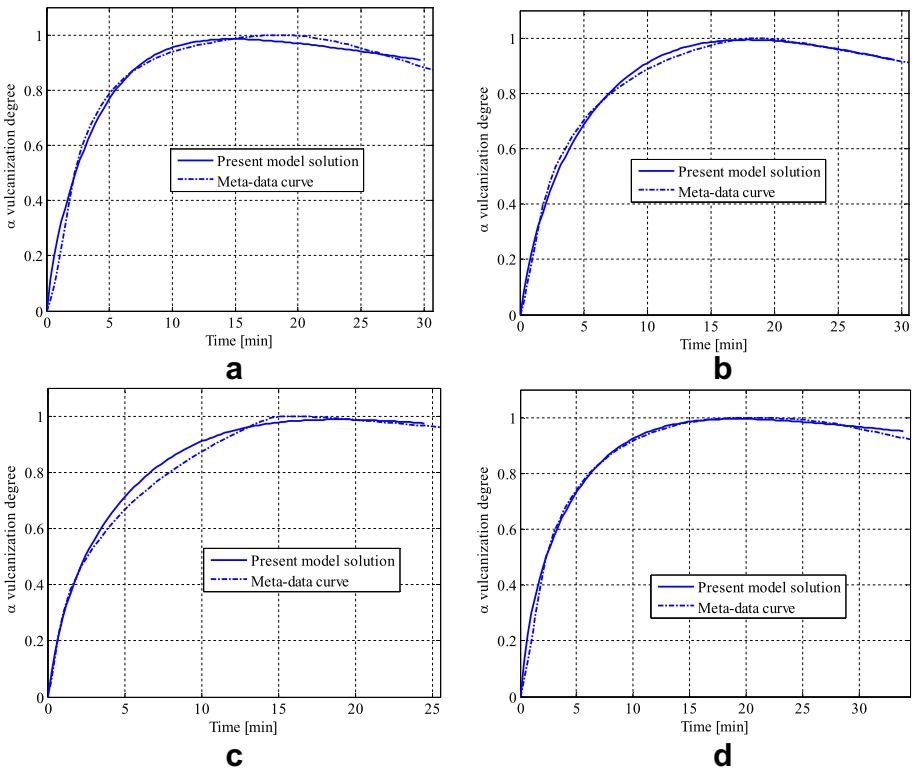

Fig. 11. Literature data set 3. a: 3-1 data set; b: 3-2 data set; c: 3-4 data set; d: 3-6 data set.

$$\frac{dS}{dt} = -K_o S \tag{8a}$$

$$\frac{dS^{*\prime}}{dt} = K_0 S - (K_1 + K_2) S^{*} \tag{8b}$$

$$\frac{dX_1}{dt} = K_1 S^{*} - K_4 X_1 \tag{8c}$$

$$\frac{dX_2}{dt} = K_2 S^{*} - K_3 X_2 \tag{8d}$$

After tedious algebra, it can be shown [23] that a closed form solution for the degree of vulcanization, intended as $\alpha = (X_1 + X_2)/S_0$, may be deduced from (8):

$$\alpha = \frac{C_4}{e^{K_4 t}} + \frac{C_6}{e^{K_3 t}} - \frac{\frac{e^{(K_3 t - K_2 t - K_1 t)}\left(C_2 K_2^2 - C_2 K_0 K_2 + C_2 K_1 K_2\right)}{K_1 + K_2 - K_3} + \frac{K_0 K_2 e^{(K_3 t - K_0 t)}}{K_0 - K_3}}{e^{K_3 t}(K_1 - K_0 + K_2)} - \\ + \frac{\frac{e^{(K_4 t - K_2 t - K_1 t)}\left(C_2 K_1^2 - C_2 K_0 K_1 + C_2 K_1 K_2\right)}{K_1 + K_2 - K_4} + \frac{K_0 K_1 S_0 e^{(K_4 t - K_0 t)}}{K_0 - K_4}}{e^{K_4 t}(K_1 - K_0 + K_2)} \tag{9}$$

with C_2, C_4 and C_6 indicating the following integration constants:

$$C_2 = -\frac{K_0}{K_1 - K_0 + K_2}$$
$$C_4 = C_2 \frac{K_1}{K_1 + K_2 - K_4} + \frac{K_1 K_0}{(K_0 - K_4)(K_1 + K_2 - K_0)} \tag{10}$$
$$C_4 = C_2 \frac{K_2}{K_1 + K_2 - K_3} + \frac{K_2 K_0}{(K_0 - K_3)(K_1 + K_2 - K_0)}$$

5. Model validation

A validation of the two-step meta-data approach was performed considering several experimental data sets available in the technical literature (see [24]) where a NR blend is vulcanized with sulphur in the presence of different accelerators at the same curing temperature (144 °C). The accelerators proved, in some cases, to give the blend excellent reversion resistance. The performance of the accelerators was comparatively estimated by collecting a minimal amount of rheometer data, as for instance times t_2 and t_{90}, reversion %, total cure time, maximum torque and some mechanical properties of the cured specimens, such as elongation at break, ultimate tensile strength and elastic modulus at 300% of elongation. Information regarding the behaviour of the blend in the rheometer chamber is particularly suited to calibrating meta-data in the first step.

The composition of the blend considered within the present validation is provided in Table 2, whereas the accelerators, together with their main properties, used for the experimental investigation are summarized in Table 3.

In Tables 4–8, a synopsis of a portion of the experimental results available in [24] and utilized in the present study is reported.

Five different experimentation sets are discussed in [24], and here some of them are re-considered to calibrate model parameters and test the reliability of the model proposed.

Some data are replicated; in particular 1-1, 2-1, 3-1 and 4-1 refer to the same accelerator, TBBS, at the same

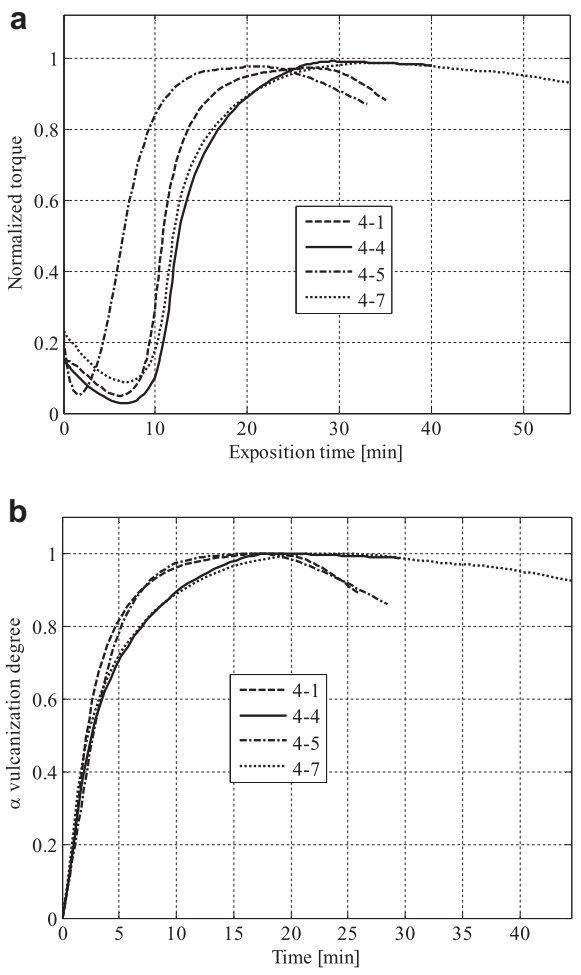

Fig. 12. Literature data set 4. a: spline meta-data; b: spline meta-data with exclusion of initial time interval before scorch.

concentration (0.6 phr), 4-7 and 5-3 to PYSSPY and 4-5 and 5-2 to MBTS.

Tables 9 and 10 summarize the experimental results used to fit constants of the numerical model. Average quantities are reported for data with multiple cure curves available. A comparison among Tables 9 and 10 and numerically obtained kinetic constants appears very straightforward (in particular t_{90} and reversion %) and allows a direct estimation of the ability of the proposed procedure to fit the experimental evidence.

In Figs. 6–15, the performance of the two-step approach proposed is graphically represented.

In particular, Figs. 6 and 7 refer to data set 1, Figs. 8 and 9 to data set 2, Figs. 10 and 11 to data set 3, Figs. 12 and 13 to data set 4, Figs. 14 and 15 to data set 5. The first figure in each set refers to the construction of the meta-model from the minimal experimental data available from the literature (first step). The normalized curve after scorch, to be used within the second step to deduce the kinetic constants, is also represented in subfigures –b.

The second figure in each set shows the performance of the kinetic model (second step) compared with the normalized meta-data (first step) deduced from the experimental values available. As can be noted, a very promising agreement was obtained for all the cases discussed, meaning that the two-step approach proposed may represent a useful automated procedure for all practitioners interested in a quick evaluation of the kinetic constants in a given blend, even when faced with very little information on the cure properties of such a material.

In some cases, the agreement appears almost perfect, with a correct estimation of both the initial curing rate and the percentage reversion. In other cases, a small but still acceptable deviation near the origin between numerical and meta-data is experienced, which appears more connected to the construction of the meta-data by means of a few experimental points instead of a lack of accuracy of the simplified mechanistic model of vulcanization proposed. The deviation from the curve to fit almost always occurs at the beginning, with the numerical model exhibiting a slightly increased curing rate. Such discrepancies may be reduced by assuming a greater first derivative for the fitting curve immediately after the scorch point in the first step.

The starting point used to initialize the non-linear least squares procedure is selected heuristically assuming no reversion ($K_3 = K_4 = 0$), considering the simplified reaction chain $A \overset{K_0}{\rightarrow} B \overset{K_1}{\rightarrow} C$ (which allows a closed form determination of concentration B) and determining the remaining kinetic constants as follows:

$$\begin{aligned} K_0 &= K_1/2 = K_2/2 \\ K_1 &= -2\ln(\beta/2)/(t_{\max} - t_2) \end{aligned} \tag{11}$$

where β is a positive coefficient less than 1 (0.2 is assumed) representing the normalized concentration of B at t_{max} (time when the maximum degree of cure is reached) and t_2 is the scorch time.

Formulas (11) are deduced mathematically in closed form, solving the differential equation system derived from reactions $A \overset{K_0}{\rightarrow} B \overset{K_1}{\rightarrow} C$.

The authors experienced sufficient robustness in the numerical approach proposed for the cases investigated, with a slow convergence rate, which required around 300–600 least squares iterations to provide the final converged solution. A starting point very near to the optimal one is found in [23], where sophisticated mathematical considerations and non-trivial algorithms were adopted that drastically improved the efficiency.

Indeed, Non-linear Least Squares method (NLS) may be affected by a lack of convergence or convergence to a suboptimal solution for difficult minimization problems and when unsuitable starting points are selected.

In order to reduce the sensitivity of least-squares fitting to outliers, a Robust least-squares Regression Method RRM was used. To minimize such an effect, a Least Absolute Residuals (LAR) method was adopted here.

The optimization procedure conducted in the second step to fit the meta-data with the mechanistic model allows an estimation of the partial kinetic constants associated with the model at the analysed curing temperature. Five constants are obtained at the end of the optimization

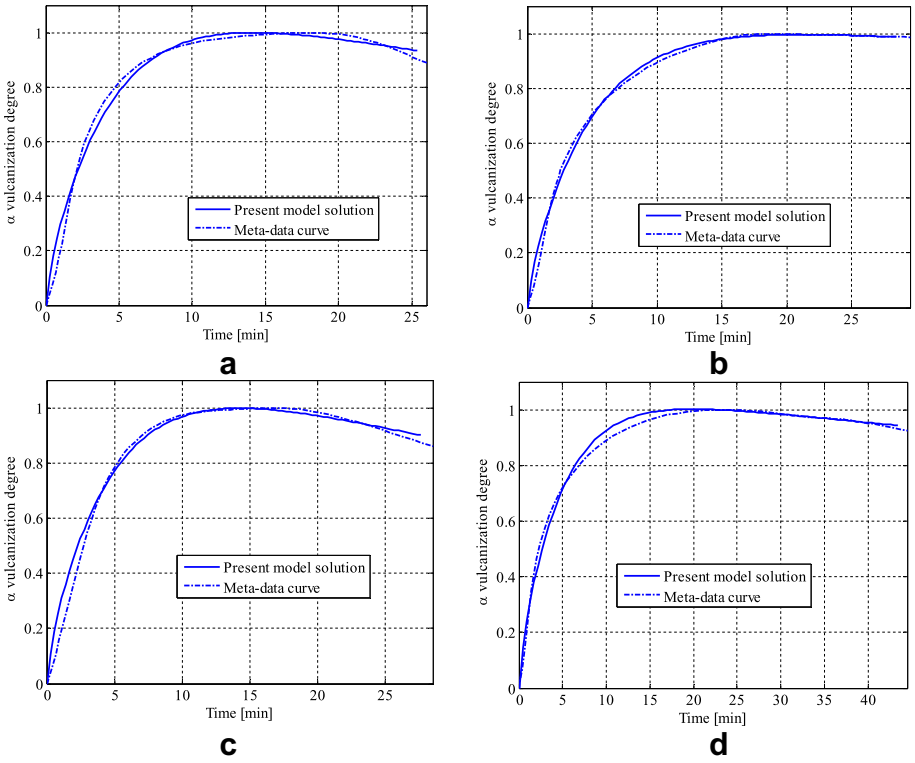

Fig. 13. Literature data set 4. a: 4-1 data set; b: 4-4 data set; c: 4-5 data set; d: 4-7 data set.

process for each numerical case discussed, which correspond to the curves that best fit the input data.

These are compared in Fig. 16; when replicated tests are present (simulations #1, #10 and #11), the average of the results obtained is reported.

Considering the hypotheses proposed for the simplified kinetic scheme adopted, it can be stated that the constant K_0 is related to the rate of formation of the activated polymer initially responsible for the crosslinking.

K_1 and K_2 proceed in parallel and have influence on the determination of t_{90} as well as on the rate at which the peak torque is reached. Finally, K_3 and K_4, again proceeding in parallel, determine the amount of reversion. It is expected that, since K_4 is linked to the breakage of single and double links, its value is significantly less than that of K_3, which is related to multiple-bond breakage.

Comparing the numerical results obtained synoptically in terms of kinetic constants (Fig. 16), as well as the experimental results available (Tables 9 and 10), the following considerations may be applied:

- MBTS appears to be the most active accelerator of all those considered in the experiments. Its increased activity results in a reduction in t_{90} (the K_1 and K_2 values provided by the numerical model are particularly large, see Fig. 16), but also in an increase in reversion, as correctly reproduced by the numerical simulations, with a large value for K_3.
- In all the simulations, K_4 values are especially low. As already mentioned, indeed, K_4 is related to the amount of reversion due to stable S-S single and double bond breaks. S-S single and double bonds are thermodynamically more stable than multiple bonds. This fact is reflected in the numerical model, where K_3 values are systematically larger than K_4 values.
- A clear trend can be deduced in the numerically obtained K_3 values. Indeed, the following ranking can be done: $K_3^1 > K_3^{10} > K_3^5 > K_3^6 \geq K_3^8 \approx K_3^2 \approx K_3^3 \approx K_3^4 \approx K_3^7 \approx K_3^9$, where the superscript indicates the # of the numerical simulation considered. The numerical values so obtained appear almost perfectly in agreement with the experimentally measured percent reversions. Cure curves 1 and 10 show particularly marked reversion, which is reproduced well by the numerical model, with peak values for the K_3 constant.
- Using the S + TBBS accelerator, there is medium reactivity with regard to formation of the active compound, with medium to high crosslinking rate but a high reversion rate. Furthermore, using S + TBBS + ZDBDP, both experimentally and numerically, a medium initial rate (reactive compound formation) and rapid crosslink formation with little reversion are experienced.
- Comparing the kinetic constants in Fig. 16 to the data in Table 9, it can be stated that the blend with accelerators PYSSPY + MBS allows medium/high vulcanization rate with a low reversion rate and optimal elasto-mechanical properties, as deduced from the values obtained experimentally for M300, UST and UE % on vulcanized items.
- From the data in Table 10 and the results in Fig. 16, it can be deduced that, using a blend with TBBS + ZDBDP

accelerators, it is possible to increase the curing rate with a slight, but still acceptable, increase in reversion, as correctly reproduced in the proposed numerical procedure. From the experimental data, it is also possible to see that the final mechanical properties of the vulcanized items (elastic modulus and tensile strength) remain within the range of acceptability for the blend under consideration.

- Using dialkyldithiophosphates (as ZDBDP), it is possible to obtain improved reversion resistance (see also the work presented in [25]). However, blends containing such accelerators generally burn slightly on the surface and this affects their practical use. ZDBDP with TBBS is an accelerator combination that drastically decreases the cure time needed, but with a very short scorch delay. With about a stoichiometric equivalent by weight of CTP, roughly the same improvements in the curing rate with very little reversion may be obtained. Finally, certain triazine derivatives have been identified as active accelerators [26]; however, increasing their proportion in the blend with the PSSR accelerator also results in superficial burns.

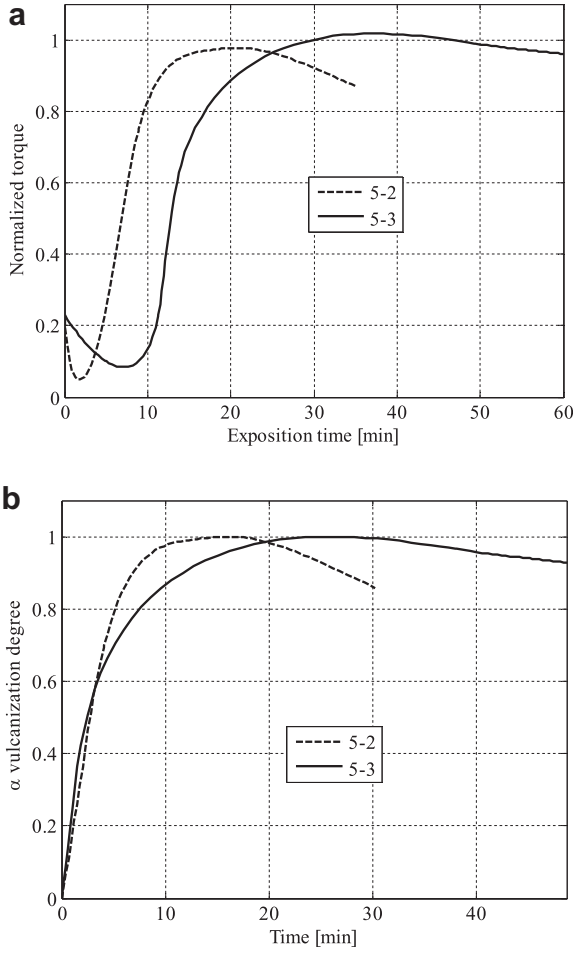

Fig. 14. Literature data set 5. a: spline meta-data; b: spline meta-data with exclusion of initial time interval before scorch.

6. Conclusions

A two-step meta-model for NR vulcanized with sulphur in a standard rheometer test has been presented.

The first step relies upon numerical rheometer curve fitting, obtained using natural cubic splines and performed using a few bits of experimental information from the cure curve, as for instance the scorch time, t_{90} and reversion percentage.

The second step is a simplified mechanistic model of vulcanization, where kinetic constants are numerically determined using a least squares procedure and assuming the cure data fit that obtained in the previous step.

The numerical procedure proposed was assessed on a number of experimental datasets available, in both the presence and absence of reversion. The model demonstrated rapid convergence and robustness, providing results in very good agreement with the experimental evidence.

The usefulness of the procedure proposed is twofold. Indeed, (1) it allows the detailed cure curve at a fixed vulcanization temperature to be deduced when only a few experimental points are available and (2) provides, within the assumed simplified kinetic scheme, partial reaction

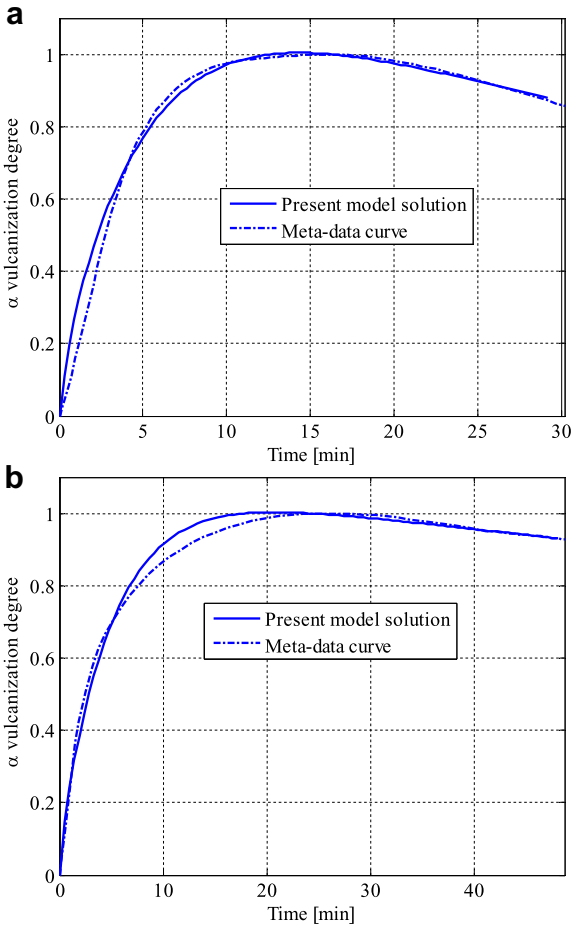

Fig. 15. Literature data set 5. a: 5-2 data set; b: 5-3 data set.

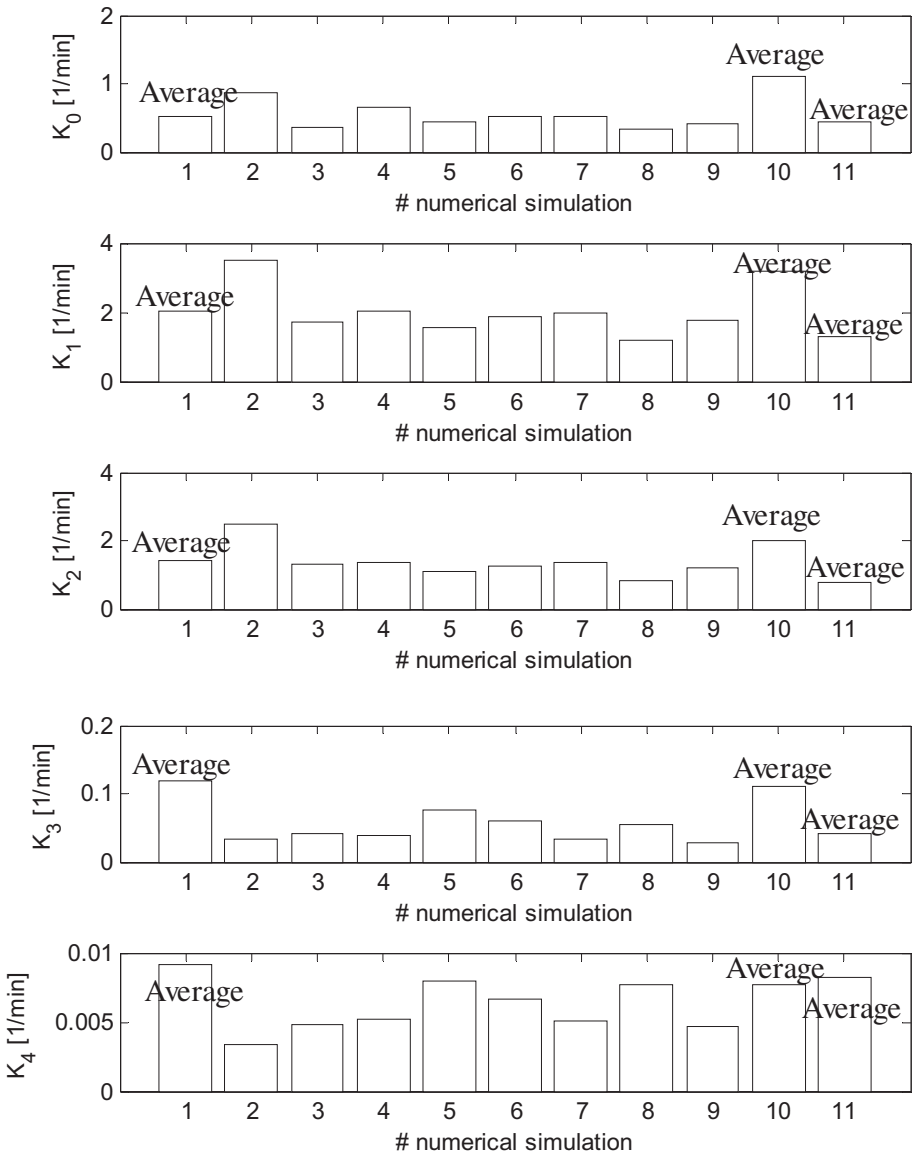

Fig. 16. Synoptic comparison between the partial kinetic constants obtained in the different cases analysed numerically.

kinetic constants. This last feature of the proposed model appears particularly interesting. Indeed, when characteristic points from two rheometer charts, corresponding to at least two different cure temperatures, are available, and Arrhenius' law is adopted for the partial kinetic constants, it is possible to numerically simulate the cure behaviour of the blend under any thermal condition and, therefore, to predict its degree of vulcanization during a real industrial vulcanization process.

References

[1] A.Y. Coran, Vulcanization, in: Science and Technology of Rubber (Chapter 7), Academic Press, New York, 1978.
[2] A.P. Rakmatullina, R.A. Akhmed'yanova, A.G. Liakumovich, Ts. B. Portnoi, E.G. Mokhnatkina, R.S. Il'yasov, Int. Polym. Sci. Technol. 31 (12) (2004) 29.
[3] S. Yamashita, T. Kaneko, Handbook of Crosslinking Agents, Taiseisha, Tokio, 1981.
[4] S. Yamashita, T. Kaneko, Handbook of Crosslinking Equipment, Taiseisha, Tokio, 1983.
[5] C. Goodyear, US Patent 3633 (1844).
[6] F.W. Billmeier Jr., Textbook of Polymer Science, third ed., John Wiley and Sons, 1984.
[7] M.L. Krejsa, J.L. Koenig, Rubber Chem. Technol. 66 (1993) 376.
[8] C.H. Chen, J.L. Koenigs, E.A. Collins, Rubber Chem. Technol. 54 (1981) 734.
[9] C.T. Loo, Polymer 15 (1974) 729.
[10] N.J. Morrison, M. Porter, Rubber Chem. Technol. 57 (1984) 63.
[11] R. Ding, I. Leonov, J. Appl. Polym. Sci. 61 (1996) 455–463.
[12] R. Ding, I. Leonov, A.Y. Coran, Rubber Chem. Technol. 69 (1996) 81.
[13] G. Milani, F. Milani, Rubber Chem. Technol. 85 (4) (2012) 590–628.
[14] G. Milani, F. Milani, J. Math. Chem. 48 (2010) 530–557.
[15] G. Milani, F. Milani, J. Appl. Polym. Sci. 119 (1) (2011) 419–437.
[16] G. Milani, F. Milani, J. Appl. Polym. Sci. 124 (2012) 311–324.
[17] G. Milani, E. Leroy, F. Milani, R. Deterre, Polym. Test. 32 (2013) 1052–1063.

[18] E. Leroy, A. Souid, R. Deterre, Polym. Test. 32 (3) (2013) 575–582.
[19] ASTM D 2084-81, Standard Test Methods for Vulcanized Rubber and Thermoplastic Elastomers-tension, Annual Book of ASTM Standards, 1986.
[20] X. Sun, A.I. Isayev, Rubber Chem. Technol. 82 (2) (2009) 149–169.
[21] A.M. Zaper, J.L. Koenig, Rubber Chem. Technol. 60 (1987) 252.
[22] I.S. Han, C.B. Chung, S.J. Kang, S.J. Kim, H.C. Chung, Polymer (Korea) 22 (1998) 223–230.
[23] G. Milani, F. Milani, Effective Closed Form Starting Point Determination for Kinetic Model Interpreting NR Vulcanized with Sulphur, Journal of Mathematical Chemistry, in press, http://dx.doi.org.10.1007/s10910-013-0272-2.
[24] L.H. Davis, A.B. Sullivan, A.Y. Coran, in: Proc.: International Rubber Conference IRC 86 – Göteborg, Sweden, vol. 2, 1986, pp. 387–392.
[25] V.V. Beresnev, V.A. Sapronov, L.A. Ognevskii, Sov. Rubber Technol. 29 (1970) 7.
[26] H. Westlinning, Rubber Chem. Technol. 43 (1970) 1194.